Atmospheric Tidal Measurements at 50 km from a Constant-Altitude Balloon

HAROLD N. BALLARD, NORMAN J. BEYERS AND BRUCE T. MIERS

Atmospheric Sciences Laboratory, U. S. Army Electronics Command, White Sands Missile Range, N. M.

AND MIGUEL IZQUIERDO AND JOHN WHITACRE

Schellenger Research Laboratories, University of Texas at El Paso

(Manuscript received 22 May 1972)

ABSTRACT

A balloon, the second in a series of high-altitude balloon flights, was launched to a record altitude of 50 km from White Sands Missile Range, N. M., on 22 September 1969. The 8.7×10^5 cubic meter, helium-filled, zero-pressure, polyethelene balloon served as a constant-level stable support for an instrument payload consisting of bead thermistor atmospheric and balloon-skin temperature sensors, thermal conductivity pressure gage, a forward-scattering beta-ray atmospheric density gage, chemiluminescent ozonesondes, a Geiger tube cosmic ray detector, and an accelerometer for the determination of the vertical component of balloon acceleration. Radar position-time data served to determine the wind velocity. Seven hours and 40 minutes of data were obtained from the various instruments at a near-constant altitude of 49 km (±1 km). This paper discusses specifically the variations in the observed balloon trajectory, the supporting rocketsonde-determined winds, and the balloon-borne temperature sensor values as related to the existence of a diurnal atmospheric tide near 50 km. It also presents the related data obtained from the other instruments comprising the payload.

1. Introduction

The term "atmospheric tide" is used to refer to atmospheric oscillations, whether gravitationally or thermally excited, whose periods are equal to or submultiples of a solar or lunar day. The tidal oscillations are superposed on the prevailing atmospheric motions.

Until approximately 10 years ago, observations related to atmospheric tides consisted of detailed studies of small tidal pressure effects at the earth's surface and inferences gained from ground-based observations of the variations in the earth's magnetic field and ionosphere. More recently, meteor trail radars (80–120 km) and rocket-borne sensors (30–80 km) are being used for the determination of winds, and are thus giving information concerning the characteristics of the atmospheric tides in the 30–120 km altitude interval.

An experimental program designed to determine the salient features of the atmospheric tides in the 30–60 km atmospheric region has been in progress since 1964 at the Atmospheric Sciences Laboratory (ASL), White Sands Missile Range (WSMR), New Mexico (Beyers and Miers, 1965; Miers, 1965; Beyers *et al.*, 1966; Beyers and Miers, 1968). This experimental program has led to the observation of variations in wind velocity and temperature in the 40–60 km altitude interval. These are thought to be related to the atmospheric tides in this region. The amplitude of the observed diurnal temperature oscillations is considerably larger than the amplitudes predicted from the theoretical considerations of Léovy (1964) and Lindzen (1967).

The details of the ASL experimental tidal program, a summary of the rather extensive studies which have been conducted to determine the proper corrections to the observed wind velocities and temperatures, and a description of other experiments which utilized independent sensing techniques to obtain comparison values of temperature-related atmospheric pressure and density, are summaried in a previous publication (Ballard *et al.*, 1970a).

This background and the progression of balloon technology to the point that it is now possible to launch a constant-altitude balloon to 50 km, coupled with the ability to predict the ensuing balloon trajectory from a study of 10 years of Meteorological Rocket Network (MRN) data, have led to two integrated-experiment balloon flights to near 50 km. The first balloon served as a stable support for a payload of six modified rocketsonde instruments and was launched on 11 September 1968 to a then record altitude of 48 km (Ballard *et al.*, 1970b; Beyers and Miers, 1970).

The second balloon served as a stable support for a payload consisting of bead thermistor atmospheric and balloon-skin temperature sensors (Ballard and Rofe, 1969), thermal conductivity pressure gauges (Thiele and Beyers, 1967), a forward-scatter beta-ray atmospheric density gage (Sellers *et al.*, 1969), chemiluminescent ozonesondes (Randhawa, 1969), a Geiger tube cosmic

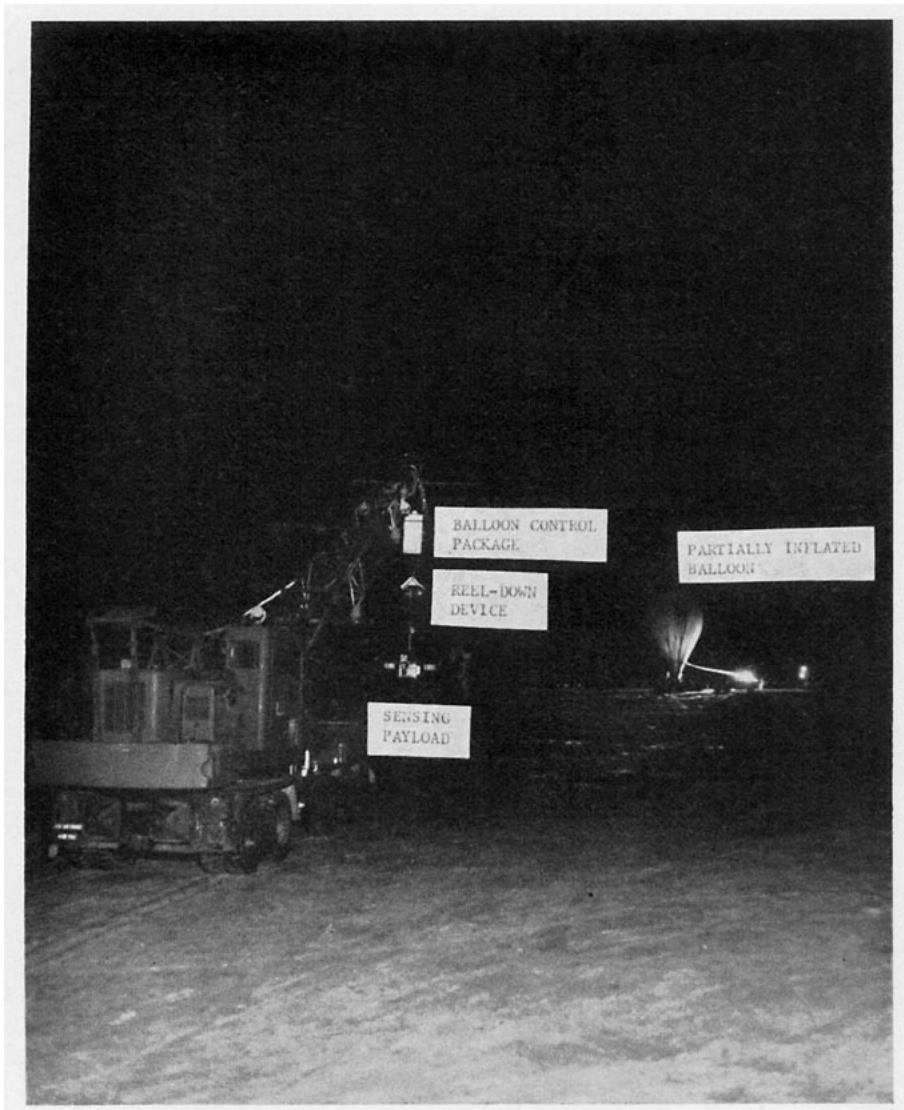

FIG. 1. Partially filled balloon and instrument package (foreground).

ray detector (Ballard *et al.*, 1970a), and an accelerometer (0.01*g* sensitivity) for the determination of the vertical component of balloon acceleration.

The balloon was launched from WSMR (32N, 106W) at 2336 MST 22 September 1969 to a new record altitude of 50 km. Atmospheric wind velocities were derived from the radar-determined balloon trajectory. This balloon flight, as was the first, was a cooperative experiment involving ASL, the Balloon Branch of U. S. Air Force Cambridge Research Laboratories, and the University of Texas at El Paso.

The research objectives of this high-altitude balloon experiment were: 1) to compare rocketsonde-measured temperatures near 50 km, after correction for known thermal effects (Ballard and Rofe, 1969), with the temperatures measured by the balloon-borne temperature sensors which were identical in configuration and sensitivity to the rocketsonde sensors, 2) to determine variations in wind and temperature near 50 km as related to the existence of a diurnal atmospheric tide, 3) to compare the beta-ray atmospheric density gage values, after correction for the cosmic ray background count, with the density values calculated from the pressure and temperature sensor measurements, 4) to determine balloon-skin temperature and balloon vertical acceleration, and 5) to determine the time variation of ozone concentration near 50 km.

2. Balloon characteristics and sensing instrument configuration

The polyethelene balloon, with a material thickness of 1.14 mm and a total expanded volume of 8.7×10^5 m^3, is shown in Fig. 1. The balloon weight was 697 kg, while the payload weight including instrument control package and radar reflector was 205 kg. There were 104 kg of ballast and 32 kg of sensing instruments. The result-

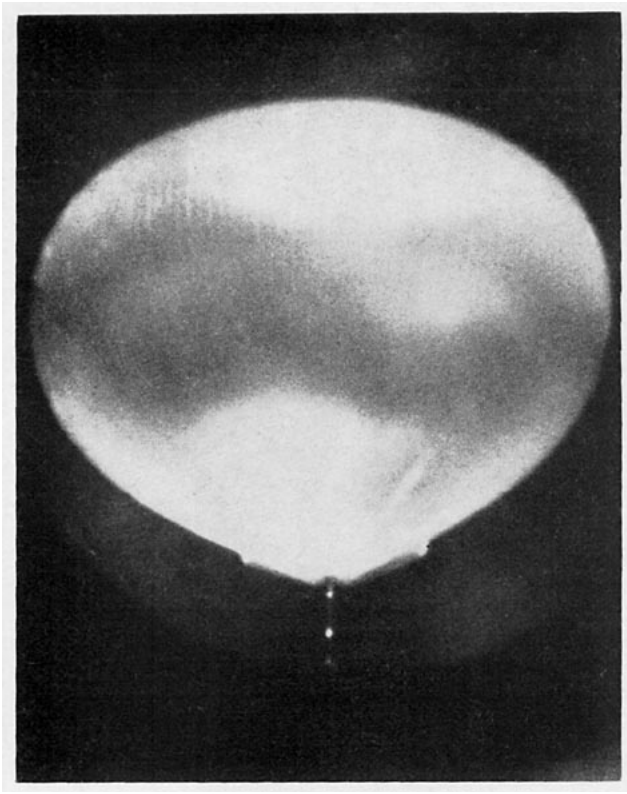

FIG. 2. Fully expanded balloon at 49 km with payload 20 m beneath the balloon.

ing free lift was 103 kg. The balloon, at the time of launching, contained approximately 573 m³ of helium at STP.

When fully expanded, near 49 km, as shown in the telescopic photograph of Fig. 2, the balloon had a mean diameter of 134 m, with the sensing payload suspended 20 m beneath the balloon. Subsequently the payload was lowered 300 m relative to this position.

Fig. 1 also presents the general configuration of the 1969 balloon flight payload (foreground) showing the balloon control package, reeldown device, and sensing payload. Electronic circuits were developed which allowed each of the eight atmospheric sensors comprising the principal payload to pulse-modulate the transmitter for a period of 30 sec out of the 4 min necessary to complete the sensor sampling cycle. Thus, each data point for a measured parameter is the average value of that parameter over a 30-sec interval. Balloon-skin temperature and balloon vertical acceleration were transmitted on another data channel with the sensing instruments mounted on the valving plate on top of the balloon (Fig. 3). The balloon-skin temperature sensor (10-mil bead thermistor) was attached to the balloon surface ~3 m from the edge of the valving plate.

3. Summary of data

The following is a listing of the data obtained from the FPS-16 radar-determined trajectory, the various balloon-borne sensors, and the rocketsonde and radiosonde temperature sensors, which were launched in support of the high-altitude balloon flight (all times are MST):

1) Projection of the radar-determined trajectory on to a horizontal plane (Fig. 4). The balloon horizontal displacement vs time data served to determine the horizontal component of the air velocity. All data from the balloon flight were obtained within a horizontal distance of the balloon launch site that did not exceed 200 km.

2) Balloon vertical acceleration as computed from the radar-determined balloon altitude as a function of time and as measured by the accelerometer. The balloon altitude was determined with an uncertainty of ±75 m. Seven hours and 40 min of data were obtained between the altitudes of 48 and 50 km, 10 hr and 20 min between 46 and 50 km, while 13 hr and 40 min of data were obtained in the 41–50 km interval.

3) Cosmic rays as related to atmosphere density measurement. The cosmic ray detector was identical in configuration and sensitivity to the beta-ray atmospheric density gauge (Betasonde) which was utilized for the direct determination of atmospheric density during the balloon flight; however, the cosmic ray detector contained no radioactive source of electrons. Thus, the measured cosmic ray background count rate, when subtracted from the total count rate of the Betasonde (scattered electrons plus cosmic rays), served to give the scattered-electron count rate. This, plus the Betasonde calibration of scattered electron count rate vs atmospheric particle number, allows one to infer the atmospheric density.

4) Atmospheric and balloon-skin temperatures as functions of time. These data, as well as the terrain profile over which the balloon floated, are presented in Figs. 5–8. The solar angle was such that, in the time

FIG. 3. Balloon-skin temperature and balloon vertical acceleration instrumentation on the valving plate.

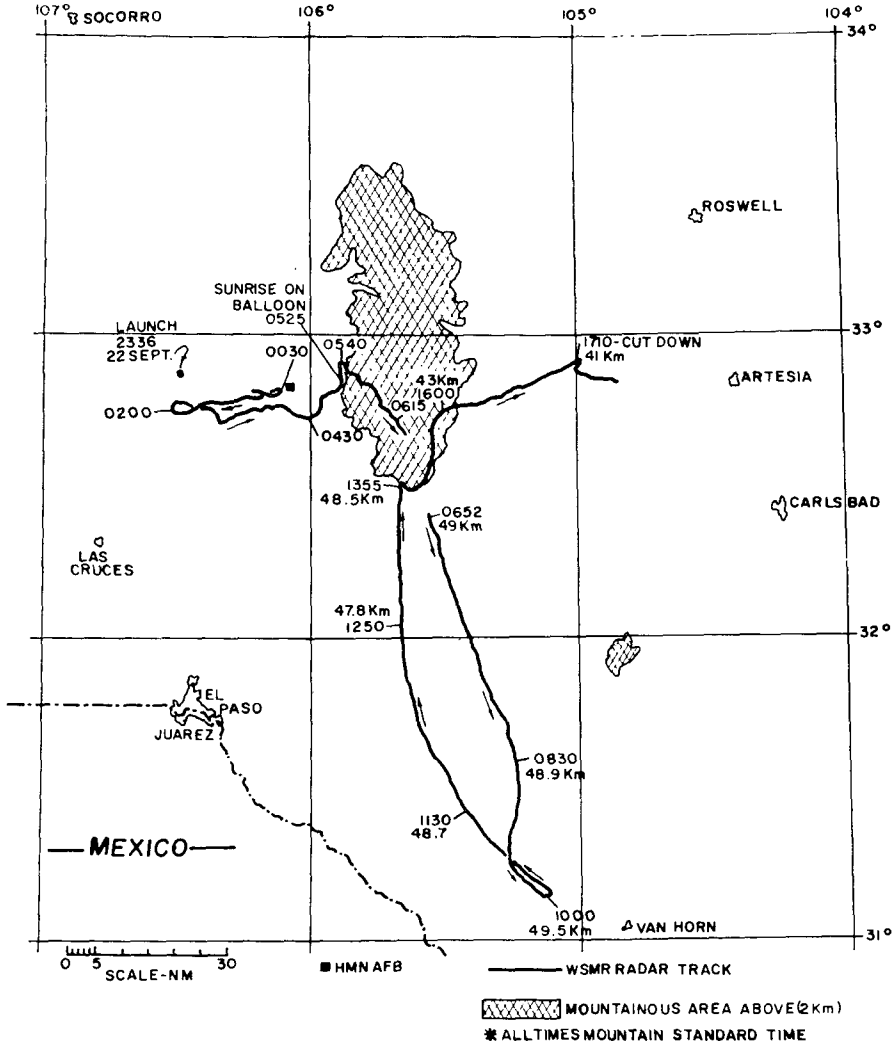

FIG. 4. Balloon horizontal trajectory.

period 0800–1355 (49±1 km), solar radiation was not directly incident upon the atmospheric temperature sensor. In addition, the sensor was mounted in such a way that infrared radiation from the balloon and instrument package was not directly incident upon it. The temperature of the balloon skin was obtained continuously from the time of balloon launching (2336, 22 September) until 0525, 23 September. It was again obtained between the times of 1100 and 1230, 23 September. The failure to determine this parameter between the times of 0525 and 1100 and between 1230 and 1710 (the latter being the time of termination of the balloon flight) was attributed to the periodic absorption by the balloon metal valving plate, in the direction of the telemetry receiver, of the telemetered signal from the instrument mounted on the valving plate at the top of the balloon (Fig. 3).

5) Atmospheric temperatures as a function of altitude as determined by rocketsonde and radiosonde temperature sensors launched in support of the high-altitude balloon flight. These data are presented in Fig. 9. Also presented in Fig. 9, for the purpose of comparison, is the atmospheric temperature vs altitude as determined from the high-altitude balloon-borne temperature sensor. This profile was obtained from the atmospheric temperature and balloon altitude vs time data of Figs. 5–8.

6) Atmospheric pressure and density as functions of time. These data are presented in Fig. 10 between 0800, the time at which the sensing payload had been lowered to a position 320 m beneath the balloon, and 1710, the time of balloon flight termination. Balloon altitude and atmospheric temperature are also shown between the same times. These figures represent a condensation of the balloon altitude and atmospheric temperature data shown in Figs. 7 and 8, after 0800, the time of completion of instrument package reel-down, when it was believed that the sensed atmospheric

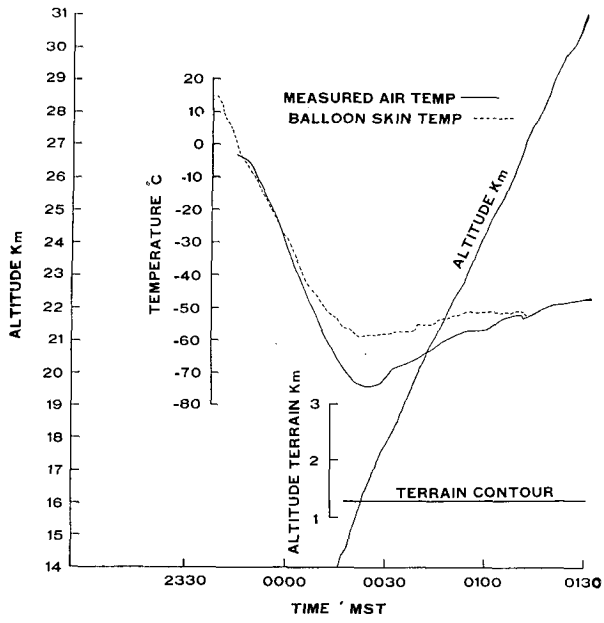

FIG. 5. Balloon altitude (14-31 km), balloon-skin temperature, and measured air temperature vs time (0015–0130).

parameters were uncontaminated by the presence of the balloon.

7) Rocketsonde and radiosonde wind data. A detailed presentation of these data, collected at WSMR in support of the high-altitude balloon flight, may be found in High Altitude Meteorological Data, World Data Center A, Vol. VI, No. 9, September 1969. From this report, the average value of the north-south (meridional) wind component in the height interval 49±1 km, the float altitude of the balloon between 0550 and 1355, was computed for the days 19–30 September 1969. The table below presents a summary of these average wind speeds:

Date (Sept. 69)	Time of rocket launching (MST)	Average north-south wind (49±1 km, m sec^{-1})
19	1200	+ 7
20	0615	− 8
22	1515	+ 6
23	0930	− 3
24	1430	+12
26	1200	+16
29	1240	+ 7
30	1145	+ 1

− From the North + From the South

8) Atmospheric ozone concentration. These data have been presented elsewhere (Randhawa, 1970).

4. Discussion of the balloon trajectory

This discussion may be omitted by the reader if he chooses to study, in detail, the data which are presented in Figs. 4–8; however, it is deemed appropriate to discuss those which appear to be the salient features of the balloon horizontal trajectory and the plot of balloon altitude as a function of time.

a. Horizontal trajectory

Had the balloon been launched on 11 September 1969, as was planned, the balloon trajectory would have been much like the 1968 balloon trajectory (Ballard *et al.*,

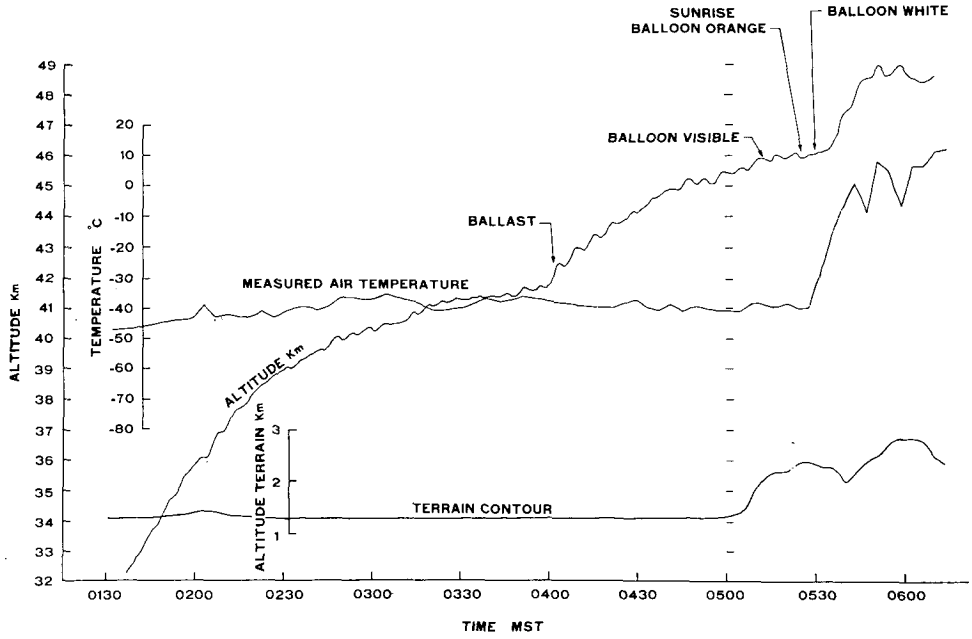

FIG. 6. Balloon altitude (32–49 km), measured air temperature, and terrain profile vs time (0130–0600).

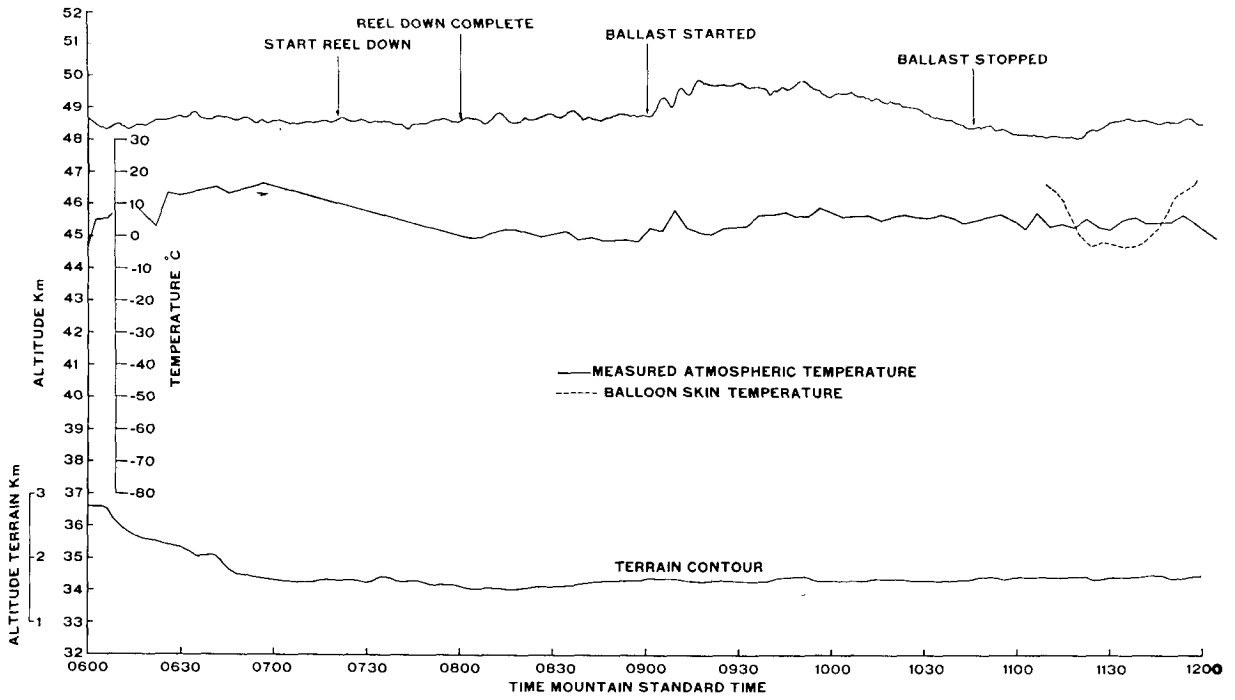

FIG. 7. Balloon altitude (49±1 km), measured temperature, balloon-skin temperature, and terrain profile vs time (0600–1200).

1970b). Thus, ground-based radars and telemetry systems were deployed for the 1969 balloon flight so that the balloon and instrument payload would be under continuous surveillance as the balloon drifted westward from its launch site at WSMR; however, because of the persistence of 1–2 m sec^{-1} surface winds at the launch site, it was not possible to launch the balloon until 22 September. The rocket soundings of the atmo-

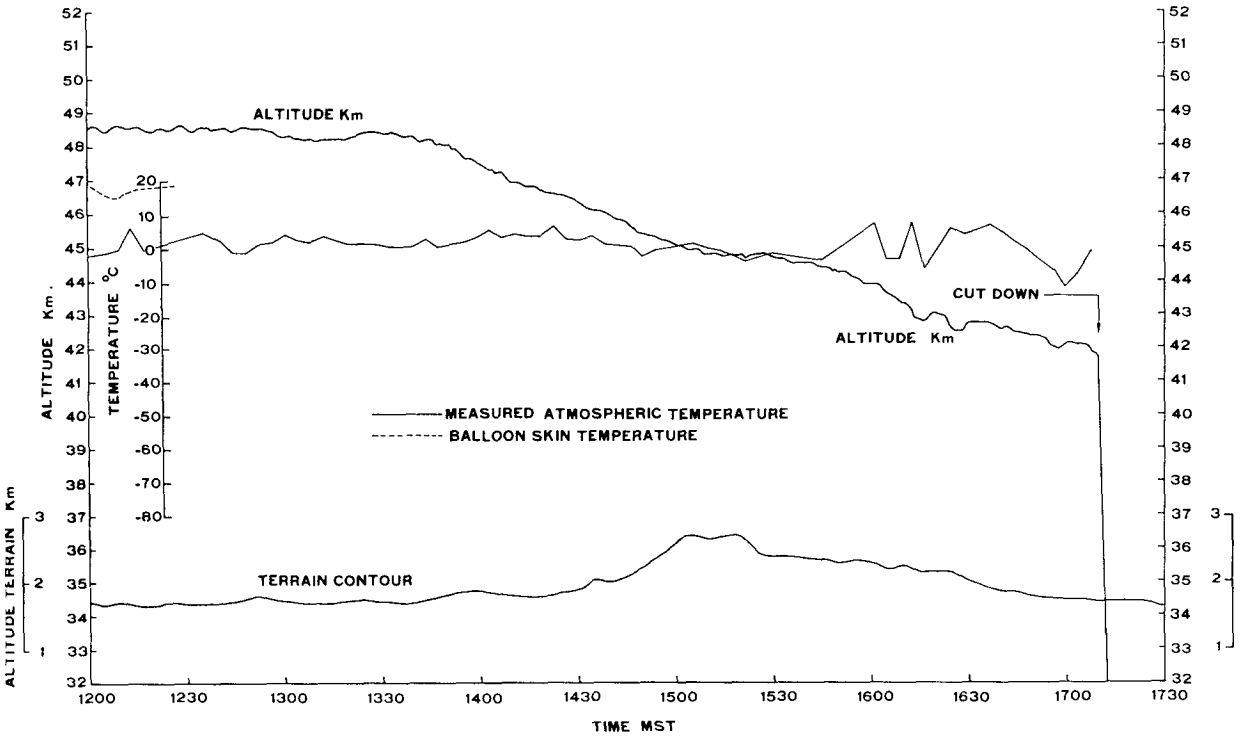

FIG. 8. Balloon altitude (48–32 km), measured atmospheric temperature, balloon-skin temperature, and terrain vs time (1200–1730)

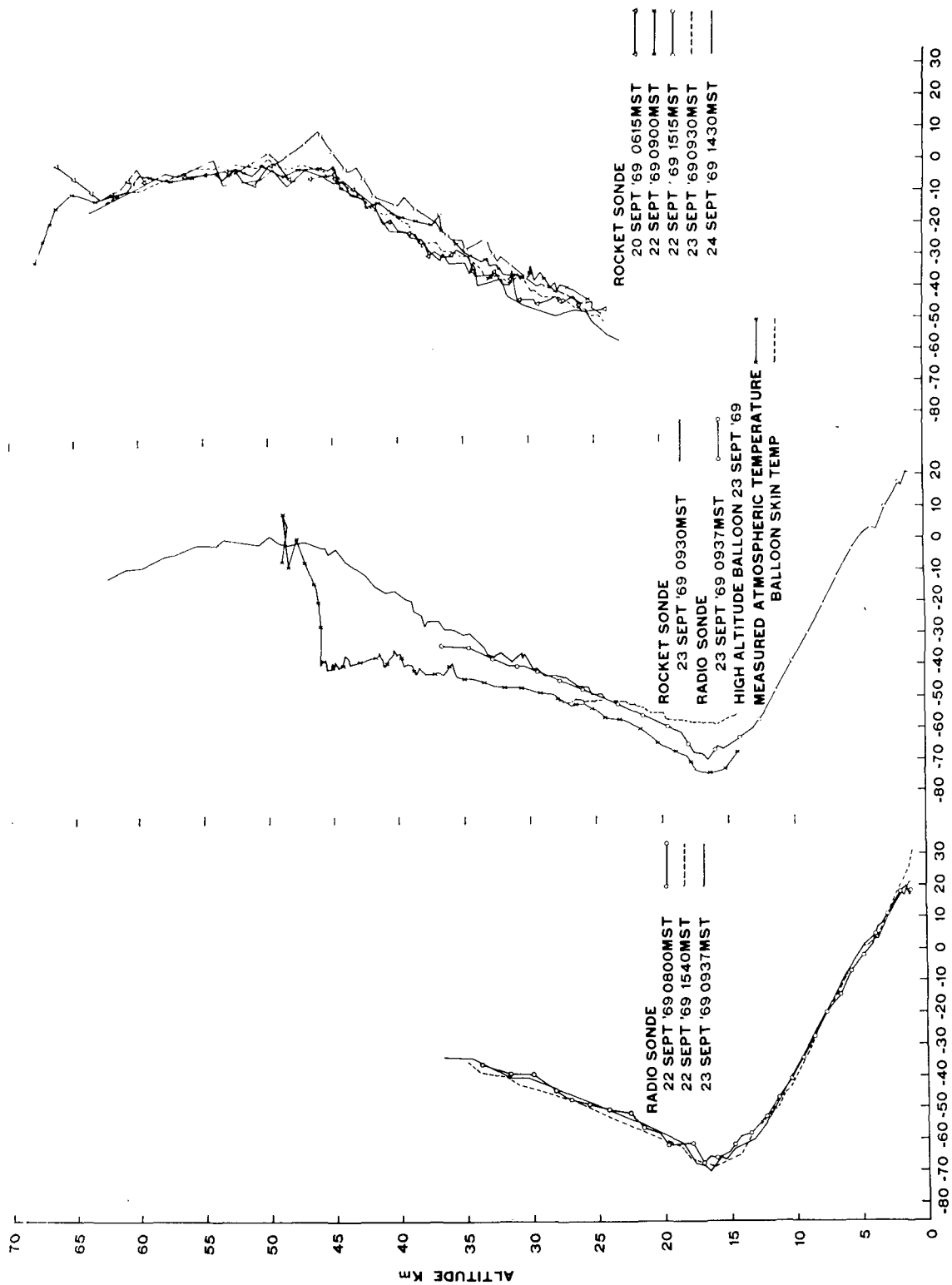

FIG. 9. Radiosonde, high-altitude balloon, and rocketsonde determined temperature profiles, 20–24 September 1969.

sphere supporting the balloon launch showed that the east-west wind component was variable around a near-zero value on 22 September with a slight predominance of winds from the west in the 30–50 km atmospheric interval. This result was in agreement with 10 years of Meteorological Rocket Network (MRN) data which show that the winds near 50 km shift from an easterly to a westerly flow in the time period 11–23 September. The decision was made to launch the balloon on 22 September even though the radar and telemetry stations placed to the west of WSMR would apparently serve no useful purpose during the experiment.

Balloon launch occurred at 2336 MST 22 September 69. The horizontal component of motion was determined by the prevailing winds up to an altitude near 46 km. Here the balloon trajectory sharply modified as evidenced by the balloon turning sharply northward (0525, 46 km) as it floated over mountainous terrain below. The balloon continued to drift northward until 0540 when it was at an altitude of 49 km, at which time it turned sharply southward and slightly eastward. It drifted from over the mountainous terrain and continued southward and slightly eastward (49.0–50.0 km) until 1000. At 1000 (49.5 km) the horizontal velocity components of the balloon suddenly reversed. From 1000–1355 (49.5–48.5 km) the balloon drifted predominately northward and slightly westward until at 1355 it came again to the mountainous terrain below, which had been encountered earlier in the day. The balloon here moved sharply toward the east and thence sharply north. After leaving the mountainous terrain at 1600 (43 km), the balloon then assumed a more eastward and slightly northward drift. The balloon flight was terminated at 1710 (41 km), a total elasped time of 17 hrs and 34 mins from the time of launching.

b. *Balloon altitude vs time*

From the time of launching, the balloon floated upward until 0130, 23 September, when it had reached an altitude of 31 km, thus having an essentially constant rate of ascent of 3.6 m sec^{-1} in this time interval (Fig. 5). From 0130–0400 the balloon ascended from 31.0 to 41.6 km at an average ascent rate of 1.2 m sec^{-1} with the rate of ascent in the last 30 min of this interval being only 0.3 m sec^{-1}. Ballast was released at 0400 with the ascent rate increasing to an average value of 0.7 m sec^{-1} from 0400–0525 (41.6–46.0 km, Fig. 6). At 0525 sunrise occurred at the balloon altitude. Shortly thereafter, at 0530, the rate of ascent increased sharply so that at 0550 the balloon reached an altitude of 49.0 km, having an average ascent rate in this interval of 2.5 m sec^{-1}. From 0550–0900 (Figs. 6 and 7) the balloon remained at altitudes between 49.0 and 48.5 km.

From 0900–1045 the remaining ballast was released. The balloon reached its maximum altitude of 50.0 km (within this time interval) at 0915. From 0915–1000 the balloon floated between the altitudes of 50.0 and 49.5 km (Fig. 7). Note from Fig. 4 that it was at 1000 that the balloon's southeastward drift shifted to northwestward. From 1000–1355 the balloon floated between 49.5 and 48.5 km (Figs. 7 and 8). At 1355 the balloon began a slow essentially monotonic descent until at 1710 (flight termination time) it reached an altitude of 41.0 km. The average descent rate in this time interval was 0.5 m sec^{-1}.

5. Results

The results derived from the various data which were obtained from the high-altitude balloon flight and supporting rocketsonde and radiosonde flights are summarized below. The numbers preceding each result correspond to those numbers in Section 3 which list and describe the data obtained.

a. (*1, 7*) *horizontal wind components*

In the time interval 0550–1000 (49$\pm$1 km), 23 September 1969, the horizontal wind components, as determined from the balloon horizontal trajectory, were from the north and west at 12.0 and 2.8 m sec^{-1}, respectively. In the time interval 1000–1355 (49$\pm$1 km), they were from the south and east at 9.6 and 2.0 m sec^{-1}, respectively. The maximum value of the north component was 19.3 m sec^{-1} at 0745 while the maximum value of the south component was 20.6 m sec^{-1} at 1300.

A study of the data presented in the table summarizing the rocketsonde-determined winds during the period 19–30 September, shows that the south–north trajectory of the balloon on 23 September was in excellent agreement with the south–north balloon trajectory which would have been predicted from these rocketsonde-determined winds at 49$\pm$1 km; that is, from 0600 to a time between 0930 and 1145 the rocketsonde-determined winds were from the north at approximately 6 m sec^{-1}. Between 0930 and 1145 the meridional component reversed to a wind from the south with an average value of $\sim$8 m sec^{-1} in the period from the time of reversal to 1515.

The south–north motion of the balloon was sharply perturbed at 1355 (48.5 km) as the balloon approached the mountainous terrain below (Fig. 4). A similar sharp deviation from the prevailing wind-induced balloon trajectory at 48 km was observed during the 1968 high-altitude balloon flight (Ballard *et al.*, 1970b) when the balloon was closely approaching mountainous (3 km MSL) terrain in Arizona. Both cases are suggestive of an orographically induced perturbation in the atmospheric flow pattern which propagated to at least 48 km. These observations are supplemented by information supplied by Gildenberg (private communication) of the Balloon Branch of AFCRL who has been associated with many high-altitude balloon flights over the past 21 years. He stated that it is typical for the balloon's trajectory to change significantly as it passes

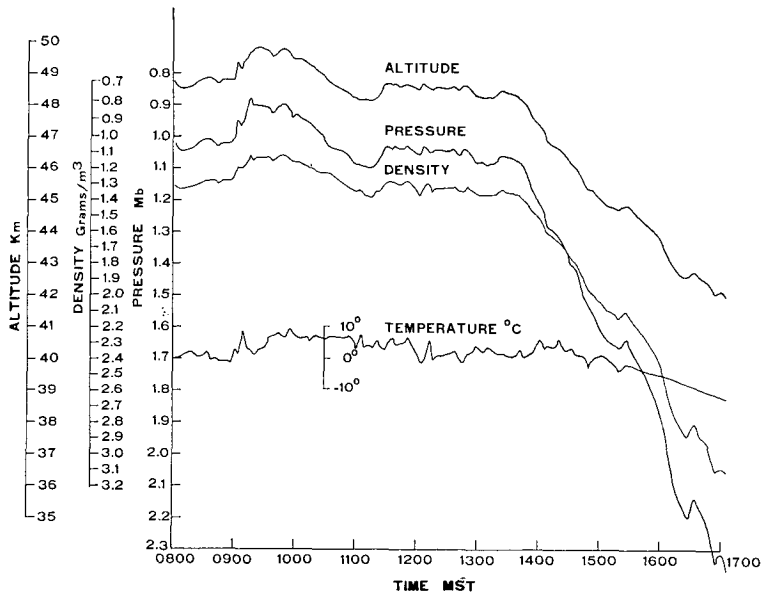

FIG. 10. Balloon altitude, atmospheric pressure, density and temperature as functions of time (0900–1700).

over, and is apparently affected by, mountainous terrain below.

b. (2) balloon vertical acceleration

The vertical acceleration of the balloon, as determined from the balloon altitude vs time data and by the accelerometer, never exceeded a value of 0.6 m sec^{-2}. This maximum value was noted at the times of ballast release and shortly after the time of sunrise at the balloon altitude.

c. (3) cosmic rays and atmospheric density

The details of this study have already been reported (Ballard *et al.*, 1970a); however, for the purpose of comparison with atmospheric density values obtained from the pressure and temperature measurements made on the high-altitude balloon payload, the Betasonde-determined density at 48.7 km, after correction for the detected cosmic rays, was 1.26×10^{-3} kg m^{-3}. The altitude of reference was chosen as 48.7 km since the balloon altitude was 48.7 km (±100 m) from 0800–0900, at 1040, and from 1130–1330.

d. (1, 4, 5) atmospheric and balloon-skin temperatures

A study of Figs. 4, 6, 7 8 and 10 shows the horizontal variability of the measured atmospheric temperature. For example, between 1150 and 1205 (Fig. 10), the measured atmospheric temperature decreased by 9C. The horizontal distance traversed by the balloon during this interval was approximately 10 km while the altitude of the balloon was 48.7 km±100 m. If it is assumed that the altitude variation of ±100 m or vertical currents did not produce the temperature change, then a horizontal temperature gradient of approximately 1C km^{-1} is implied. Beyers and Miers (1970) observed a similar horizontal temperature gradient of 0.7C km^{-1} during the 1968 balloon flight.

A study of Figs. 5, 6 and 9 shows the expected influence of the colder-than-atmosphere balloon on the measured temperatures when the sensing payload was 20 m beneath the balloon. Specifically. when the balloon was at an altitude of 28 km (0115, Fig. 5) the indicated air temperature and the balloon-skin temperature came to the same value of −51C. At 46 km (0525, Fig. 6), just before sunrise, both of the sensors registered a temperature of −40C. The 0930 rocketsonde-determined atmospheric temperatures at 28 and 46 km (Fig. 9) were −45 and −3C, respectively.

At and after the time of sunrise at the balloon altitude (0525, Fig. 6) the effect of the hotter-than-atmosphere balloon on the indicated atmospheric temperature is evident. It is particularly well illustrated between the times of 0700 and 0800 (Fig. 7) when the sensing payload was lowered to 320 m beneath the balloon. Here the indicated air temperature decreased from 19C to 0C with the balloon altitude remaining constant at 48.7 km during and after the time of reel-down. It is also indicated immediately after 0900 (Fig. 7), when, due to ballast release, the balloon altitude increased from 48.7 to 50 km. The temperature sensor 320 m below the balloon was pulled into the wake of the balloon by the 1.3 km increase in altitude, as evidenced by an apparent increase in the atmospheric temperature of +10C. The indicated air temperature then decreased to +1C when the balloon was again stable at 50 km.

For these reasons, only the atmospheric temperature

data which were obtained by the high-altitude balloon-borne sensor after the completion of instrument package reel-down (0800, Fig. 7) and when the balloon was floating stably at a given altitude are considered in the comparison of the rocketsonde-sensor-measured temperatures with the balloon-borne-sensor-measured temperatures and in the determination of the diurnal temperature variation.

Relative to the temperature sensor comparison, at 0920 and 0930 (Figs. 7 and 10), the balloon was floating at an altitude of 50 km. The air temperatures registered by the balloon-borne sensor at these times were +1C and +3C, respectively. The balloon travelled a horizontal distance of ~5 km in this 10-min interval. The temperature registered by the 0930 rocketsonde sensor at an altitude of 50 km, but at a space point approximately 100 km from the balloon-borne sensor, was 0C.

Other comparison of the temperatures measured by the radiosonde, rocketsonde, and high-altitude balloon-borne sensors (Fig. 9) give, at an altitude of 16.5 km (tropopause), −72C by the radiosonde sensor and −74C by the balloon-borne sensor. The air temperature at 28 km, as determined by a radiosonde and a rocketsonde launched at 0937 and 0930, respectively, was −45C.

In attempting to determine the magnitude of the diurnal temperature variation, a constant-altitude line at 48.7 km was drawn on the balloon altitude vs time data shown in Figs. 7 and 8. This was done between the times of 0800, when instrument package reel-down was complete, and 1330, when the balloon began its monotonic descent. This established that the balloon was at 48.7 km (±100 m) at the times 0800–0900, 1040, and 1130–1330. Between the times 0800–0900 (Fig. 7), the atmospheric temperature was slightly variable at 0C; at 1040, 1130 and 1150 it was +7C. To this point an indication of the magnitude of the diurnal temperature variation would appear to have been established. Unfortunately, as related to the diurnal temperature variation, and as discussed above with respect to the atmospheric temperature horizontal variability, between the times of 1150 and 1205 the air temperature decreased from +7 to −2C. This decrease was followed by a sharp increase to +8C at 1215 and a sharp decrease to 0C at 1230. From 1230–1330 the temperature was slightly variable at +1C.

Relative to horizontal temperature variability, note also the large atmospheric temperature oscillations (1530–1700, Fig. 8) which were observed when the balloon was floating between 45 and 43 km over the mountainous terrain as perhaps related to the sharp change in the balloon trajectory at 1355 (Fig. 4) as the balloon approached the mountainous terrain.

No plausible explanation has been found for the large variation in the balloon-skin temperature, observed in the time interval 1100–1200 (Fig. 7), without an associated large variation in the temperature measured by the atmospheric temperature sensor located 464 m below the balloon-skin temperature sensor. It was established through the calibration signal built into the balloon-skin temperature instrument that the instrument was functioning properly and that the indicated temperatures were not erroneous. A study of solar angles, relative to the mounting position of the sensor on the balloon skin during the times the skin temperature sensor indicated a 19C decrease in temperature, shows that the sensor could not have been shaded from directly incident solar radiation through a rotation of the balloon. Contrarily, the change in altitude of the balloon from 48.0 km at 1120 to an altitude of 48.7 km at 1130 is compatible with the balloon and balloon-skin temperature sensor moving into an atmospheric region of lower temperature.

e. (6) atmospheric pressure and density

The atmospheric pressure at 48.7 km (Fig. 10), as determined by the thermal conductivity gage which was part of the balloon-borne payload, was 1.02 mb. The nominal pressure given at 48.0 km by the 1966 Standard Atmosphere for the fall months, between the latitudes of 30 and 60N, is 1.023 mb.

The atmospheric density at 48.7 km, as calculated through the perfect gas equation of state from the pressure and temperature values determined by the balloon-borne sensor, was 1.28×10^{-3} kg m^{-3}. The 1966 Standard Atmosphere value at 49 km is 1.163×10^{-3} kg m^{-3}.

6. Conclusions

Based upon the statement in the introduction concerning the experimental objectives of the 22 September 1969 high-altitude balloon flight, the summary of the data obtained from the flight, and the corresponding listing of results derived from the data, the following conclusions are drawn:

1) The meridional winds determined from the high-altitude balloon flight and the supporting rocket soundings near an altitude of 49 km are in general agreement with previous experimental and theoretical results. The time of wind reversal from a north to a south flow occurred at 1000 MST, with the maximum speed from the south being 20 m sec^{-1} at 1300 MST.

Beyers *et al.* (1968) analyzed the wind data obtained from the rocket soundings of the stratosphere and lower mesosphere in tidal experiments conducted during February 1964, November 1964, July 1965, and October 1965. All four experiments showed that the maximum wind from the south at 49 km occurred between the times of 1000 and 1200 MST, with the October and November experiments giving average maximum speeds of 7.5 and 8.5 m sec^{-1}, respectively. The times of reversal of the meridional wind component from a north

wind to a south wind, for the October 1965 tidal experiment, were 0500 for a 4 km thick layer centered at 48 km and 0900 for a 4 km thick layer centered at 52 km.

The experimental results of Reed *et al.* (1969), which were derived from the analysis of 763 rocketsonde observations of the atmosphere from WSMR (32N) and Cape Kennedy (28N), showed the maximum wind from the south at 49 km occurred at 1200 LST at an average maximum speed of 8 m sec^{-1}.

These experimental results are in agreement with the theoretical atmospheric tidal wind results of Lindzen (1967) who predicts at 49 km (30N) at 1200 LST a maximum wind from the south with an average speed of 8 m sec^{-1}.

Thus, the conclusion is made that the south-north motion of the high-altitude balloon at 49±1 km on 23 September 1969, resulted from the winds associated with the atmospheric diurnal tide near 49 km with the meridional average wind speeds determined from the balloon trajectory (11 m sec^{-1}) being somewhat greater than the average values of wind speed calculated from many rocketsonde observations (8 m sec^{-1}). In addition, the time of reversal determined by the balloon trajectory occurred somewhat later (~3 hr) than the average time of reversal determined from the many rocketsonde observations.

The conclusion is also made that the south-to-north tide-related motion of the balloon was sharply perturbed at 1355 (48.5 km) as the balloon closely approached the mountainous terrain below (Fig. 4).

2) The vertical acceleration of the balloon was very small throughout the flight with maximum values of acceleration (0.6 m sec^{-2}) occurring at the times of ballast release and shortly after the time of sunrise at the balloon altitude.

3) The balloon-borne observed electron forward-scatter atmospheric density gage count-rate values, when properly corrected for the count rate caused by detected cosmic rays near 49 km, gave an atmospheric density value at 48.7 km which was within 6% of 1.28×10^{-3} kg m^{-3} as calculated through the perfect gas equation of state from the balloon-borne pressure and temperature sensor values at the same altitude. Based upon this comparison, the conclusion is made that with proper instrument redesign, the Betasonde can serve as a useful tool to give direct measurements of atmospheric density to an altitude of 90 km.

4) The atmospheric thermal structure at 48.7 km, the altitude of reference for temperature vs time comparisons during the balloon flight, shows considerable horizontal variability. The maximum horizontal temperature gradient observed at this altitude during the experiment was approximately 1C km^{-1}. Because of this horizontal variability no definite conclusion could be drawn concerning the value of the diurnal temperature variation associated with the thermal tide.

The balloon-skin temperature was found to be approximately 10–12C warmer than the observed atmospheric temperature when the solar radiation was incident upon the balloon. This conclusion is in agreement with that drawn from the 1968 high-altitude flight.

5) The high-altitude balloon-borne atmospheric temperature sensor values at 50 km at 0920 and 0930 were +1 and +3C, respectively, at two space points separated by a horizontal distance of 5 km. The temperature at 50 km, as determined from the 23 September rocketsonde launched at 0930, was 0C at a space point approximately 100 km from the balloon-borne temperature sensor.

The conclusion is made that the agreement between the two sensors was excellent, and perhaps even fortuitous, in light of the observed atmospheric horizontal thermal variability at the stratopause level. Also, in the region of data overlap up to an altitude of 35 km (Fig. 9), the temperatures determined by the radiosonde rod thermistor launched at 0937 are in excellent agreement with the temperatures determined by the rocketsonde 10-mil bead thermistor launched at 0930. This difference between the sensors at altitudes above 35 km usually begins to mainfest itself clearly at an altitude of approximately 25 km.

REFERENCES

Ballard, H. N., and B. Rofe, 1969: The thermistor measurement of temperature in the 30–65 km atmospheric region. *Stratospheric Circulation*, Vol. 22, *Progress Series Amer. Inst. Aeronaut. Astronaut.* New York, Academic Press, 141–166.

——, M. Izquierdo, J. Smith and J. Whitacre, 1970a: Corrections to observed atmospheric densitometer values as caused by cosmic rays. *J. Appl. Meteor.*, **9**, 933–939.

——, N. J. Beyers, M. Izquierdo and J. Whitacre, 1970b: A constant altitude balloon experiment at 48 kilometers. *J. Geophys. Res.*, **75**, 3501–3512.

Beyers, N. J., and B. T. Miers, 1965: Diurnal change in the atmosphere between 30 and 60 km over White Sands Missile Range. *J. Atmos. Sci.*, **22**, 262–266.

——, and ——, 1968. A tidal experiment in the equatorial stratopause over Ascension Island. *J. Atmos. Sci.*, **25**, 155–159.

——, and ——, 1970: Measurement from a zero-pressure balloon in the stratopause (48 km). *J. Geophys. Res.*, **75**, 3513–3522.

——, —— and R. J. Reed, 1966: Diurnal tidal motions near the stratopause during 48 hours at White Sands missile range. *J. Atmos. Sci.*, **23**, 325–333.

——, —— and E. P. Avara, 1968: The diurnal tide near the stratopause over White Sands missile range. Tech. Rept. ECOM-5180, Atmos. Sci. Lab., U. S. Army Electronics Command, White Sands Missile Range, N. M., 20 pp.

Leovy, C., 1964: Radiative equilibrium in the mesosphere. *J. Atmos. Sci.*, **21**, 238–248.

Lindzen, R. S., 1967: Thermally driven tides in the atmosphere. *Quart. J. Roy. Meteor. Soc.*, **93**, 18–42.

Miers, B. T., 1965: Wind oscillations between 30 and 60 km over White Sands missile range, New Mexico. *J. Atmos. Sci.*, **22**, 382–387.

Randhawa, J. S., 1969: Ozone measurements from a stable platform near the stratopause level. *J. Geophys. Res.*, **74**, 4588–4590.

——, 1970: A balloon measurement of ozone near sunrise. Tech. Rept. ECOM-5300, Atmos. Sci. Lab., U. S. Army Electronics Command, White Sands Missile Range, N. M., 8 pp.

Reed, J. R., M. J. Oard and Marga Siemmski, 1969: A comparison of observed and theoretical diurnal tidal motions between 30 and 60 kilometers. *Mon. Wea. Rev.*, **97**, 456–459.

Sellers, B., H. N. Ballard and M. Izquierdo, 1969: Direct measurement of air density in the 30–60 kilometer region by beta-ray forward scattering. *Intern. J. Radiat. Isotopes*, **20**, 341–351.

Thiele, O. W., and N. J. Beyers, 1967: Upper atmospheric pressure measurements with thermal conductivity gauges. *J. Atmos. Sci.*, **24**, 551–557.